PCCP

PAPER

View Article Online
View Journal | View Issue



Cite this: *Phys. Chem. Chem. Phys.*, 2016, **18**, 2054

# Strong room-temperature blue-violet photoluminescence of multiferroic $BaMnF_4$

Shuang Zhou,[a] Yakui Weng,[a] Zhangting Wu,[a] Jinlong Wang,[d] Lingzhi Wu,[e] Zhenhua Ni,[ab] Qingyu Xu*[abcf] and Shuai Dong*[a]

Received 30th September 2015,
Accepted 3rd December 2015

DOI: 10.1039/c5cp05864c

www.rsc.org/pccp

$BaMnF_4$ microsheets have been prepared using a hydrothermal method. Strong room-temperature blue-violet photoluminescence has been observed (an absolute luminescence quantum yield of 67%) with two peaks located at 385 nm and 410 nm. More interestingly, photon self-absorption phenomenon has been observed, leading to an unusual abrupt decrease in the luminescence intensity at a wavelength of 400 nm. To understand the underlying mechanism of such emission, the electronic structure of $BaMnF_4$ has been studied using first principles calculations. The observed two peaks are attributed to electron transitions between the upper-Hubbard bands of the Mn's $t_{2g}$ orbitals and the lower-Hubbard bands of the Mn's $e_g$ orbitals. The Mott gap mediated d–d orbital transitions may provide additional degrees of freedom to tune the photon generation and absorption in ferroelectrics.

## 1. Introduction

Materials that can efficiently emit blue and violet light have attracted a lot of research attention over the past few decades due to their wide range of applications. For example, blue light-emitting materials are used in light-emitting diodes (LEDs) for full-color displays and in semiconductor laser diodes (LDs) for optical communication systems. Violet-light-emitting materials are used in digital versatile disks (DVDs) for higher storage capacity and in LDs for undersea optical communications. As we all know, the most common inorganic fluorescent phosphors are alkaline earth metal sulfides (ZnS, CaS)[1–3] and aluminates ($SrAl_2O_4$, $CaAl_2O_4$ $BaAl_2O_4$)[4–6] as a matrix, with the rare earth as an activating agent or activator. When comparing with these two categories, solid inorganic fluorides have high optical transparency, lower phonon energy, high ionicity, electron-acceptor behavior and anionic conductivity,[7–9] and also have a wide range of promising optical applications in optics, biological labels and lenses.[10,11] Most inorganic fluorides phosphors need rare earth elements as an activator. In addition, complex preparation technology and toxic properties hinder their applications to a certain degree. In contrast, transition metal fluorides synthesized using a simple and low-cost fabrication process seems to be more economical and environmentally friendly. In this study, a hydrothermal method was performed and the room-temperature photoluminescence (PL) of a selected inorganic multiferroic fluoride, $BaMnF_4$, has been studied both experimentally and by first principles calculations.

$BaMnF_4$ belongs to the family of $BaMF_4$-type fluorides (M = Mn, Fe, Co, Ni, Mg, and Zn), which share the same orthorhombic structure. $BaMnF_4$ can be described by the non-centrosymmetric space group $A2_1am$, in which $Ba^{2+}$ ions are layered with sheets of distorted corner-sharing $[MnF_6]^{2-}$ octahedra, as shown in the inset of Fig. 1.[12] It has attracted considerable research interest due to its multiferroic properties, which possess a large spontaneous polarization along the *a*-axis up to 11.5 μC $cm^{-2}$ [13] and antiferromagnetism with the magnetic moment roughly along the *b*-axis simultaneously.[14,15] Such a multiferroic nature provides the possibility to tune the physical properties of $BMnF_4$ *via* magnetic/electric stimulation. In addition, just like other inorganic fluorides, $BaMnF_4$ can also be applied towards the manufacture of scintillators, high resolution color displays, white light-emission devices, security labels, monitoring equipment, and cancer therapy drugs.[16–18]

Despite its intensively studied multiferroic properties, investigations on the optical properties of $BaMnF_4$ are rather rare,[19] especially at room temperature. One possible reason is that the fluorides are much more difficult to synthesize when compared with widely studied oxides. In addition, $BaMnF_4$ has a structural phase transition occurring at 247 K and a magnetic transition at

[a] *Department of Physics, Southeast University, Nanjing 211189, China. E-mail: xuqingyu@seu.edu.cn, sdong@seu.edu.cn*
[b] *Key Laboratory of MEMS of the Ministry of Education, Southeast University, Nanjing 210096, China*
[c] *Collaborative Innovation Center of Suzhou Nano Science and Technology, Soochow University, Suzhou 215123, China*
[d] *School of Optoelectronic Engineering, Nanjing University of Posts and Telecommunications, Nanjing 210023, China*
[e] *School of Geography and Biological Information, Nanjing University of Posts and Telecommunications, Nanjing 210023, China*
[f] *National Laboratory of Solid State Microstructures, Nanjing University, Nanjing 210093, China*

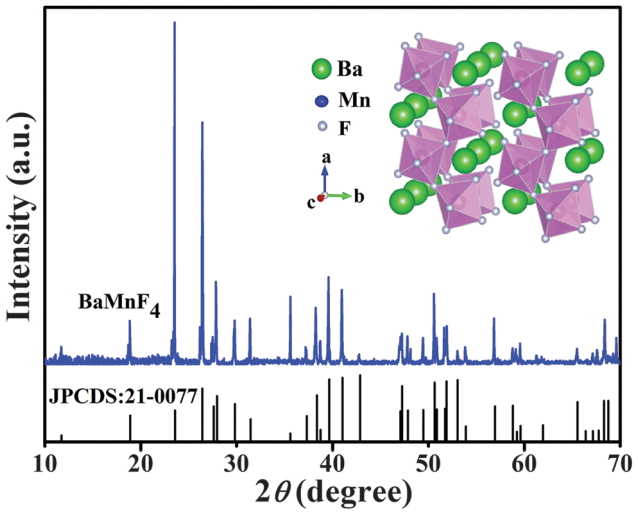


Fig. 1 The XRD pattern of $BaMnF_4$ microsheets synthesized using the hydrothermal method (main plot). The schematic crystal structure of $BaMnF_4$ (inset).

26 K,[20,21] which may influence its optical behavior. Even though, the luminescence spectra of $BaMnF_4$ at a wavelength in the red and near infrared range were studied by Goldberg *et al.* more than thirty years ago, the emission bands at 600 nm, 640 nm, and 720 nm were observed at low temperature (10–110 K), but they did not mention its properties at room temperature.[21]

In this study, $BaMnF_4$ microsheets have been grown using a hydrothermal method and the room temperature PL in the blue-violet region have been investigated when excited with ultra-violet light. Two strong emission bands have been clearly observed; the strongest position located at a wavelength of 385 nm and the other at 410 nm. The photoluminescence excitation (PLE) spectra show a stable luminescent phenomenon for the two peaks. More interestingly, an unusual drop of luminescence intensity at 400 nm has been observed, which was confirmed to be attributed to the photon self-absorption effect. Furthermore, the underlying mechanism of PL has been explained as a Mott-gaped d–d transition according to first-principles electronic structure calculations.

## 2. Experimental and methods

A pale pink powder of $BaMnF_4$ microsheets was synthesized using a hydrothermal method.[22,23] Stoichiometric $BaF_2$ and $Mn(CH_3COO)_2{\cdot}4H_2O$ were mixed, dissolved in trifluoroacetic acid solution (volume ratio of $CF_3COOH$ and $H_2O$ is 1 : 2) and the diluted solution contained in a polytetrafluoroethylene autoclave, heated to 220 °C, held for 20 h, and then cooled slowly to room temperature. After discarding the upper remaining liquid, the product was washed with ethanol and dried in vacuum conditions. All the reagents were used as starting materials without further purification.

The equipment used to characterize the structure and morphology of the prepared sample is as follows: X-ray diffraction (XRD, Rigaku Smartlab3) with Cu Kα radiation, transmission electron microscope (TEM, Tecnai F20) and scanning electron microscope (SEM, FEI Inspection F50). The PL and PLE were measured using a spectrofluorometer (fluorolog3-TCSPC, Horiba Jobin Yvon). Absorption measurements were carried out with a spectrophotometer (UV-3600) and the fluorescence efficiency (characterized as the absolute quantum yield) was recorded on an Edinburgh FLS920P spectrometer with an integrating sphere.

The first-principles density function theory (DFT) calculations were performed using the spin-polarized local density approximation (LDA) method with Hubbard $U$ correction, based on the projector-augmented wave (PAW) potentials, as implemented in the Vienna ab initio Simulation Package (VASP).[24,25] Various values of the effective Hubbard coefficient ($U_{eff} = U - J$) on Mn's 3d states have been tested from 0 eV to 4 eV.[26–28] The cutoff energy of the plane-wave was 550 eV and the $k$-point mesh is $\Gamma$-centered 5 × 7 × 5. The experimental lattice constants and internal atomic positions were adopted in the following calculation as the initial values,[20] which are fully optimized till the Hellmann–Feynman forces converged to less than 0.01 eV $Å^{-1}$. The experimental antiferromagnetism was adopted.[29]

## 3. Results and discussion

The structural and sample quality of our $BaMnF_4$ powder were checked by XRD, as shown in Fig. 1, which confirms the orthorhombic structure with space group of $A2_1am$. No impurity phase can be detected from the XRD pattern. A schematic crystal structure of $BaMnF_4$ is sketched in the inset plot of Fig. 1 wherein the sheet structure consists of distorted corner-sharing $[MnF_6]^{2-}$ octahedra. The morphology of our microcrystals was studied using SEM images at different magnifications as shown in Fig. 2(a and b). The banded sheets have a regular shape and the lateral size is of several micrometers. This micro-sheet morphology suggests an anisotropic growth under hydrothermal conditions, which should be related to the layered-like crystal structure. The inset of Fig. 2(b) shows the selected area electron diffraction (SAED) pattern obtained by TEM, which is good evidence that the crystals were micro-sized single crystals of good quality.

The $BaMnF_4$ powder was pressed into a thin circular tablet for luminescence measurements. During the measurements for

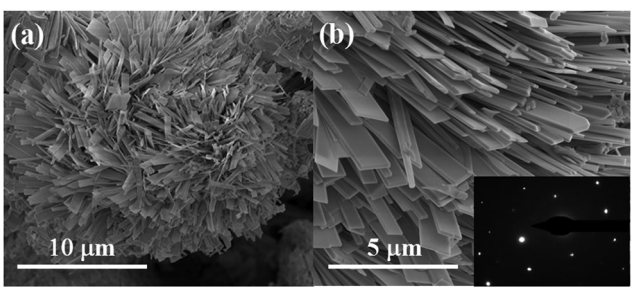


Fig. 2 (a and b) SEM images at different magnifications of the $BaMnF_4$ microsheets. Inset of (b): The SAED pattern of a single crystal obtained by TEM.

PL and PLE, small gratings of 2 nm were used for both the incident and emergent light detectors. Fig. 3(a) shows the PL spectra with various excitation wavelengths ($\lambda_{exc}$ = 260–360 nm). All these spectra show similar shapes, containing two main emission bands. These two strongest emission positions were located at 385 nm and 410 nm. The peak positions of the luminescence spectra are robust and almost unchanged when the excitation wavelength was tuned. With various excitation light, the PL spectrum excited using 280 nm ultra-violet light had the strongest intensity, *i.e.* the optimal excitation wavelength. The two emission peaks have a large linewidth, which may be due to a broad distribution of the particle size or strong electron–phonon coupling of the multiferroics.[30] Furthermore, the fluorescence emission spectrum at 78 K (inset of Fig. 3(a)) shows the same behavior with that found at room temperature, *i.e.* two peaks and a valley at identical positions, which suggests the luminescence behavior of $BaMnF_4$ is temperature-independent, at least between 78 K and room temperature.

Fig. 3(b) shows the PLE spectra of $BaMnF_4$ excited with light at wavelengths in the range of 235 and 340 nm. The emission intensities at both the wavelengths at 385 nm and 410 nm were monitored. The PLE intensity at 385 nm was higher than that found at 410 nm, which was consistent with the aforementioned PL spectra. The inset of Fig. 3(b) shows the luminescent image of the $BaMnF_4$ powder excited with ultraviolet light. The bright blue color was due to the selectivity of the naked eye. The fluorescence efficient of the $BaMnF_4$ was measured using an integrating sphere and its absolute luminescence quantum yield (300–520 nm) reached ~67% and this was quite a high value for an inorganic fluoride phosphor.

In contrast to the general overlapping shape of the two neighboring emission bands,[31] a sudden drop in the PL intensity at the wavelength of 400 nm can be clearly observed in Fig. 3(a), which may be due to a photon self-absorption mechanism,[32] which will be discussed later. This absorption was robust and unvaried with the excitation wavelength in the range of 260–360 nm.

The proposed interpretation of luminescence can be further checked by first-principles calculations. By varying the Hubbard coefficient, it was found that $U_{eff}$ = 1 eV gives the best description for the $BaMnF_4$. The local magnetic moment within the Wigner–Seitz sphere was 4.49 $\mu_B$ per Mn atom, implying the high-spin state for $Mn^{2+}$, as expected. The density of state (DOS) and projected density of states (PDOS) show that the electronic bands

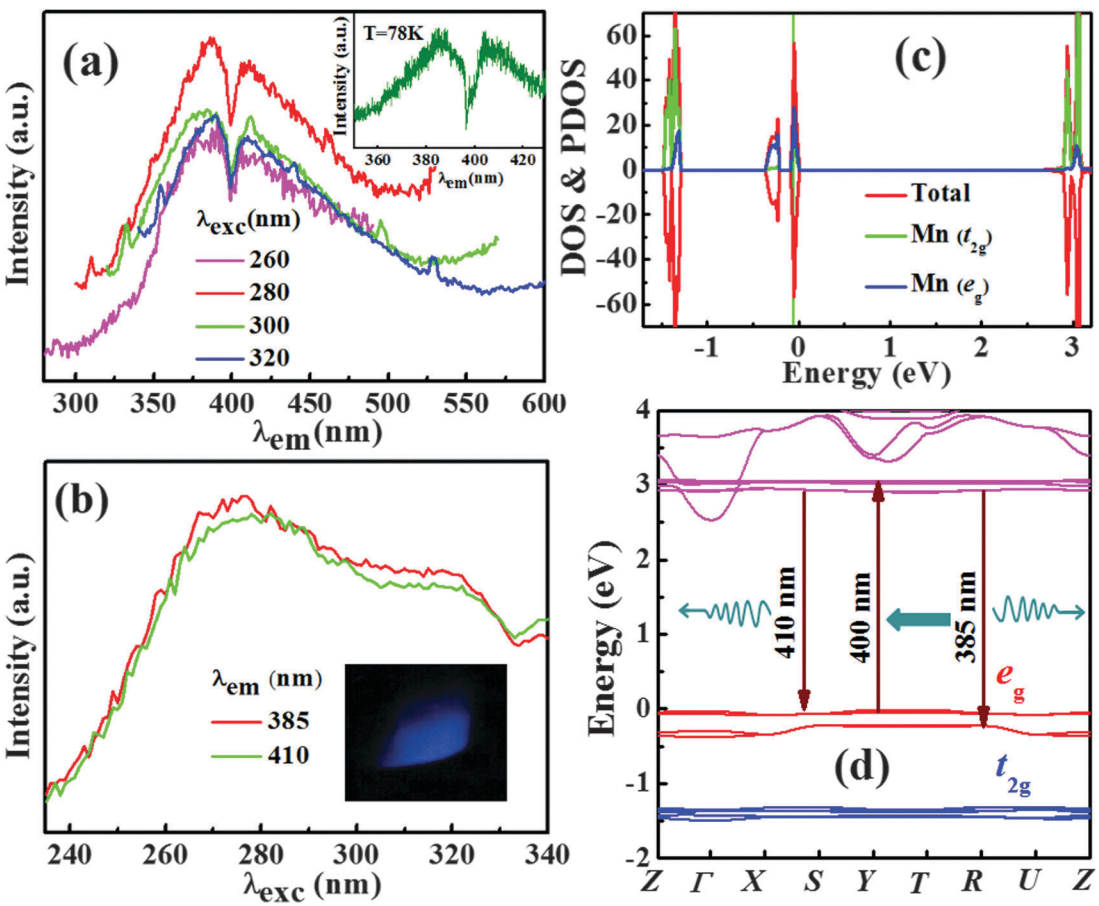


Fig. 3 (a) The PL spectra of $BaMnF_4$ under various excitations; the inset shows the PL spectra excited by a 325 nm laser at 78 K; (b) the PLE spectra with an emission wavelength of 385 nm and 410 nm; the inset shows the image of $BaMnF_4$ powder under ultraviolet illumination; (c) DOS of $BaMnF_4$. The orbital-resolved PDOS is also calculated and the five 3d orbitals grouped into two categories (the triplet $t_{2g}$: $d_{xy}$, $d_{yz}$, $d_{xz}$ and the doublet $e_g$: $d_{x^2-y^2}$, $d_{3z^2-r^2}$). (d) The band structures. The arrows denote the mechanism of PL emission and self-absorption.

 

near the Fermi level are from the Mn 3d orbitals, as shown in Fig. 3(c). A non-trivial character of $BaMnF_4$'s electronic structure was that both the $t_{2g}$ and $e_g$ bands are very narrow, implying an extremely localized 3d state. This localization was partially due to the half-filling fact of Mn's 3d orbital, which was the most ideal condition for Mottness. Another reason was the weak hybridization between the Mn 3d orbitals and the F 2p orbitals whose energy was much lower.

The band gap of $BaMnF_4$ in our DFT calculation was about 3.0 eV (when $U_{eff}$ = 1 eV), separating the empty upper-Hubbard $t_{2g}$ bands and occupied lower-Hubbard $e_g$ bands. This Mott gap coincides with the emission photon energy, suggesting a d–d transition induced PL. It is well known that the intrashell photon excitation/emission is usually quite weak due to the selection rule. In this sense, however, the quantum yield of $BaMnF_4$ was as high as 67% (300–520 nm), suggesting that the strong room temperature PL of $BaMnF_4$ observed here was quite prominent considering the fact that no rare earth element was involved. Noting that the spontaneous ferroelectric polarization of $BaMnF_4$ distorts the lattice and changes the symmetry of the electronic wavefunctions, which may be responsible for the violation of the selection rule as proposed for ideal isolated atoms.

To reveal more information on the sudden drop of intensity at 400 nm, the absorption spectrum of $BaMnF_4$ powder was measured ranging from 300 nm to 550 nm, as shown in Fig. 4(a). The conspicuous peaks (A–E) of absorption are summarized in Table 1. Our results for the absorption agrees with the previous unpolarized absorption spectrum of a single crystal of $BaMnF_4$ that also shows a sharp peak at 400 nm at 295 K.[32] Comparing the peaks of our experimental spectra and those reported in the literature,[33] it is clear that all the peaks nearly have the same photon energy. This was also powerful evidence for the sample quality of the $BaMnF_4$ prepared. Furthermore, Fig. 4(b) shows the contrast figure between the PL spectra excited with 280 nm (red) and inverted absorption (green). It was obvious that the strong absorption peak at 400 nm fits well with the deep valley of the PL, both for the same shape and exact position. In addition, the PLE shown in Fig. 3(b) presents a similar two peak phenomenon. To date, the proposed self-absorption has been confirmed

Table 1 Information on the main peaks A–E corresponding to the absorption spectrum shown in Fig. 4(a). The data presented in the second column are taken from ref. 33

| Peak | Photon energy ($10^3$ $cm^{-1}$)[33] | Photon energy ($10^3$ $cm^{-1}$) | Wavelength (nm) | Energy (eV) |
|---|---|---|---|---|
| A | 19.15 | 19.20 | 520.8 | 2.38 |
| B | 23.05 | 23.18 | 431.4 | 2.87 |
| C | 25.22 | 25.00 | 400.0 | 3.10 |
| D | 28.00 | 28.33 | 353.0 | 3.51 |
| E | 30.05 | 29.68 | 336.9 | 3.68 |

rationally. Self-absorption is a common case for solid luminescent materials and has been researched for many years.[32,34–38] In some solid states, physical phenomena, such as multiple scattering and self-absorption of the emitted light may occur, leading to the distortion or splitting of the luminescence features, thus compromising the data interpretation.[32,39] In our system, the two detached peaks in the PL spectra should originally belong to a broad peak with large line width. However, because of the self-absorption effect at 400 nm, the broad peak was divided into two parts.

According to the DFT band structure (Fig. 3(d)), both the $e_g$ bands and $t_{2g}$ bands are further split due to the Jahn–Teller distortion of the Mn-$F_6$ octahedra. Especially, for the $e_g$ ones, the split was about 0.1 eV. By considering such splitting, the two peaks of emission and the self-absorption can be well mapped to the transitions among these sub-bands, as indicated in Fig. 3(d). First, the electrons are excited to the unoccupied upper-Hubbard $t_{2g}$ orbitals by the exciting ultraviolet light, then the transition of the excited electrons from unoccupied $t_{2g}$ orbitals to the split $e_g$ orbitals leads to the PL emissions at 385 nm and 410 nm. The emission photons can be absorbed and the electrons in the upper $e_g$ orbitals are excited to the upper unoccupied $t_{2g}$ orbitals, leading to the deep valley at 400 nm in the PL spectra.

## 4. Conclusions and perspective

$BaMnF_4$ microsheets were synthesized using a hydrothermal method and the PL and PLE spectra at room temperature

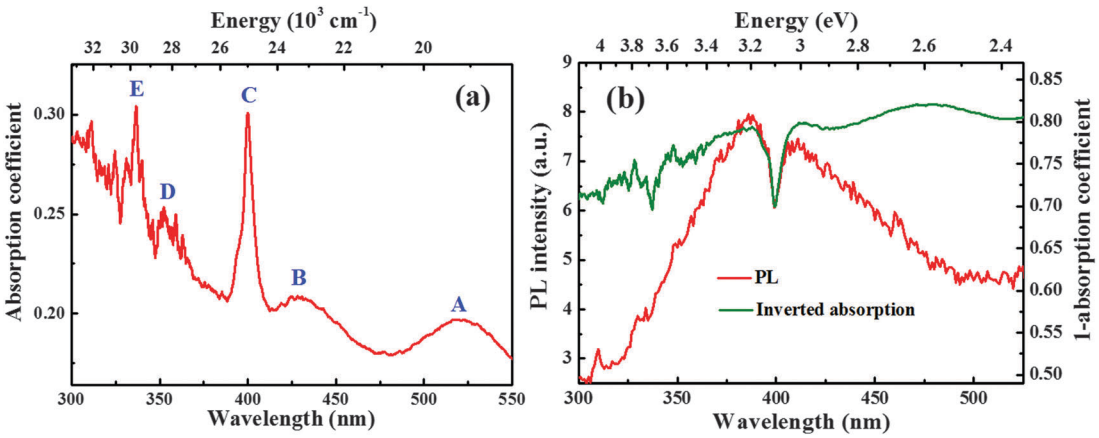


Fig. 4 (a) The absorption spectra of $BaMnF_4$. (b) A comparison between the PL spectra excited at 280 nm (red) and the inverted absorption (green).

studied. Strong emissions at 385 nm and 410 nm can be excited by ultraviolet illumination with wavelengths ranging from 260 nm to 340 nm with 280 nm found to be the most efficient excitation wavelength. By comparing the absorption spectra and PL spectra, it was confirmed that the sudden decrease in the PL spectra at 400 nm was induced by the self-absorption effect. According to first-principles calculations, the emissions were mainly due to the d–d transitions between the split $t_{2g}$ and $e_g$ orbitals by both the Hubbard repulsion as well as the Jahn–Teller distortion of the $[MnF_6]^{2-}$ octahedra in the $BaMnF_4$. Because both the Hubbard bands and Jahn–Teller distortion can be tuned by many methods, *e.g.* doping or strain, the strong room temperature PL of $BaMnF_4$ has potential to be tuned for better applications, which will be studied in the future.

## Acknowledgements

This study is supported by the National Natural Science Foundation of China (51172044, 51471085, and 51322206) and the Natural Science Foundation of Jiangsu Province of China (BK20151400).

## References

1 J. K. Cooper, S. Gul, S. A. Lindley, J. Yano and J. Z. Zhang, *ACS Appl. Mater. Interfaces*, 2015, **7**, 10055.
2 X. L. Wang, J. Y. Shi, Z. C. Feng, M. R. Li and C. Li, *Phys. Chem. Chem. Phys.*, 2011, **13**, 4715.
3 M. Georgin, L. Carlini, D. Cooper, S. E. Bradforth and J. L. Nadeau, *Phys. Chem. Chem. Phys.*, 2013, **15**, 10418.
4 A. A. Yaremchenko, V. V. Kharton, A. A. Valente, S. A. Veniaminov, V. D. Belyaev, V. A. Sobyanin and F. M. B. Marques, *Phys. Chem. Chem. Phys.*, 2007, **9**, 2744.
5 F. Clabau, X. Rocquefelte, S. Jobic, P. Deniard, M. H. Whangbo, A. Garcia and T. Le Mercier, *Chem. Mater.*, 2005, **17**, 3904.
6 S. H. Jua, U. S. Oha, J. C. Choia, H. L. Parka, T. W. Kimb and C. D. Kimc, *Mater. Res. Bull.*, 2000, **35**, 1831.
7 C. Feldmann, M. Roming and K. Trampert, *Small*, 2006, **2**, 1248.
8 Z. W. Quan, D. M. Yang, P. P. Yang, X. M. Zhang, H. Z. Lian, X. M. Liu and J. Lin, *Inorg. Chem.*, 2008, **47**, 9509.
9 P. Gao, Y. Xie and Z. Li, *Eur. J. Inorg. Chem.*, 2006, 3261.
10 Y. B. Mao, F. Zhang and S. S. Wong, *Adv. Mater.*, 2006, **18**, 1895.
11 W. S. Wang, L. Zhen, C. Y. Xu, J. Z. Chen and W. Z. Shao, *ACS Appl. Mater. Interfaces*, 2009, **1**, 780.
12 C. Ederer and N. Spaldin, *Phys. Rev. B: Condens. Matter Mater. Phys.*, 2006, **74**, 024102.
13 L. F. David and J. F. Scott, *J. Phys. C: Solid State Phys.*, 1977, **10**, L329.
14 P. Sciau, M. Clin, J. P. Rivera and H. Schmid, *Ferroelectrics*, 1989, **105**, 201.
15 D. E. Cox, S. M. Shapiro, M. Eibschiitz, H. J. Guggenheim and R. A. Cowley, *Phys. Rev. B: Condens. Matter Mater. Phys.*, 1979, **19**, 5754.
16 M. C. Marco de Lucas, M. Moreno, F. Rodriguez and P. G. Baranov, *J. Phys.: Condens. Matter*, 1996, **8**, 2457.
17 S. F. Lim, W. S. Ryu and R. H. Austin, *Opt. Express*, 2010, **18**, 2309.
18 X. Yang, S. Xiao, J. W. Ding and X. H. Yan, *J. Mater. Sci.*, 2007, **42**, 7042.
19 C. Li and J. Lin, *J. Mater. Chem.*, 2010, **20**, 6831.
20 V. Franco-Puntes, K. M. Krishnan and A. P. Alivisatos, *Science*, 2001, **291**, 2115.
21 V. Goldberg, D. Pacheco, R. Moncorge and B. Di Bartolo, *J. Lumin.*, 1979, **18**, 143.
22 S. W. Kim, H. Y. Chang and P. S. Halasyamani, *J. Am. Chem. Soc.*, 2010, **132**, 17684.
23 S. Zhou, J. Wang, X. F. Chang, S. B. Wang, B. Qian, Z. D. Han, Q. Y. Xu, J. Du, P. Wang and S. Dong, *Sci. Rep.*, 2015, **5**, 18392.
24 G. Kresse and J. Hafner, *Phys. Rev. B: Condens. Matter Mater. Phys.*, 1993, **47**, 558.
25 G. Kresse and J. Furthmuller, *Phys. Rev. B: Condens. Matter Mater. Phys.*, 1996, **54**, 11169.
26 M. Cococcioni and S. D. Gironcoli, *Phys. Rev. B: Condens. Matter Mater. Phys.*, 2005, **71**, 035105.
27 T. Hashimoto, S. Ishibashi and K. Terakura, *Phys. Rev. B: Condens. Matter Mater. Phys.*, 2010, **82**, 079903.
28 S. Dong, W. Li, X. Huang and E. Dagotto, *J. Appl. Phys.*, 2014, **115**, 17D723.
29 D. E. Cox, M. Eibschutz, H. J. Guggenheim and L. Holmes, *J. Appl. Phys.*, 1970, **41**, 943.
30 A. Endoh, Y. Nakata, Y. Sugiyama, M. Takatsu and N. Yokoyama, *Jpn. J. Appl. Phys.*, 1998, **38**, 1085.
31 L. Liu, D. M. Zhang, Y. S. Zhang, Z. G. Bao and L. F. Chen, *J. Mater. Sci.*, 2013, **48**, 876.
32 C. Clementi, C. Miliani, G. Verri, S. Sotiropoulou, A. Romani, B. G. Brunetti and A. Sgamellotti, *Appl. Spectrosc.*, 2009, **63**, 1323.
33 T. Tsuboi and W. Kleemann, *Phys. Rev. B: Condens. Matter Mater. Phys.*, 1983, **27**, 3762.
34 C. Clementi, F. Rosi, A. Romani, R. Vivani, B. G. Brunetti and C. Miliani, *Appl. Spectrosc.*, 2012, **66**, 1233.
35 K. Suzuki, A. Kobayashi, S. Kaneko, K. Takehira, T. Yoshihara, H. Ishida, Y. Shiina, S. Oishi and S. Tobita, *Phys. Chem. Chem. Phys.*, 2009, **11**, 9850.
36 T. S. Ahn, R. O. Al-Kaysi, A. M. Muller, K. M. Wentz and C. J. Bardeen, *Rev. Sci. Instrum.*, 2007, **78**, 086105.
37 N. Kaihovirta, G. Longo, L. Gil-Escrig, H. J. Bolink and L. Edman, *Appl. Phys. Lett.*, 2015, **106**, 103502.
38 G. Verri, C. Clementi, D. Comelli, S. Cather and F. Pique, *Appl. Spectrosc.*, 2008, **62**, 1295.
39 T. Suhasini, B. C. Jamalaiah, T. Chengaiah, S. J. Kumar and R. L. Moorthy, *Physica B*, 2012, **407**, 523.

 